Liu *et al. Chem Synth* 2024;4:10
DOI: 10.20517/cs.2021.51

Chemical Synthesis

Supplementary Material

Facile synthesis of heteroporous covalent organic frameworks with dual linkages: a "three-in-one" strategy

Le Liu[1], Xi Su[1], Meiling Qi[1], Xinyue Gao[2], Hao Ren[2,*], Long Chen[1,*]

[1]State Key Laboratory of Supramolecular Structure and Materials, College of Chemistry, Jilin University, Changchun 130012, Jilin, China.
[2]State Key Laboratory of Inorganic Synthesis and Preparative Chemistry, College of Chemistry, Jilin University, Changchun 130012, Jilin, China.

[*]**Correspondence to:** Prof. Long Chen, State Key Laboratory of Supramolecular Structure and Materials, College of Chemistry, Jilin University, 2699 Qianjin Street, Changchun 130012, Jilin, China. E-mail: longchen@jlu.edu.cn; Prof. Hao Ren, State Key Laboratory of Inorganic Synthesis and Preparative Chemistry, College of Chemistry, Jilin University, 2699 Qianjin Street, Changchun, 130012, China. E-mail: renhao@jlu.edu.cn

Contents

Section 1. Materials and Methods

Materials

1,3,5-Tribromobenzene (98%), 4-formylphenylboronic acid (98%), *p*-toluenesulfonic acid (98%), 2,2-dimethyl-1,3-propanediol (98%), 4-aminophenylboronicacidpinacolester (98%), 1,4-phenylenebisboronic acid (98%), methylboronic acid (97%), bis(pinacolato)diboron (98%) were purchased from Heowns. $Pd(PPh_3)_4$ (99.9%) and $Pd(PPh_3)_2Cl_2$ (99.99%) were purchased from 3A Chemicals. Ethyl acetate (EA), dichloromethane (DCM), petroleum ether (PE), *N,N*-Diisopropylethylamine (DIPEA), 1,4-dioxane, toluene, mesitylene, 1-Butanol (*n*-BuOH) and 1,2-dichlorobenzene (*o*-DCB) were purchased from Aladdin reagent. All commercial available chemicals were directly used as received without further purification.

Physical measurements

^1H NMR and ^{13}C NMR were recorded on Bruker AVANCE III-400MHz NMR spectrometer. ^{13}C CP/MAS NMR spectra were recorded with the contact time of 2 ms (ramp 100) and a pulse delay of 3 s with a 4-mm double resonance probe. Fourier transform infrared (FT-IR) spectra were recorded in transmission mode on a Bruker Alpha spectrometer using KBr pellets with a scan range of 400-4000 cm^{-1}. Elemental analyses were performed by Elementar Vario EL III. The thermal stabilities of the two COFs were evaluated by Thermogravimetric analysis (TGA) on a differential thermal analysis instrument (TA instruments TGA-Q50-1918 analyzer) ranging from room temperature to 800 °C with the interval of 10 °C/min under N_2 atmosphere using an empty Al_2O_3 crucible as the reference. The Powder X-ray diffraction (PXRD) patterns of the two COFs were recorded on X-ray diffractometer (RIGAKU SMARTLAB 9KW) or DX-27mini (400W) X-Ray diffractometer with a Cu target tube and a graphite monochromator. Field emission scanning electron microscopies (FE-SEM) were performed on a Hitachi SU8010 microscope operating at an accelerating voltage of 3.0 kV. Surface areas and pore size distribution were measured via a Specific surface area and pore size analyzer (ipore 400) by drying samples at 100 °C for 12 hours under vacuum (10^{-5} bar) before analysis, and pore size distribution was calculated by nonlocal density functional theory (NLDFT). The simulated PXRD patterns were determined by the Reflex module. Pawley refinement of the experimental PXRD of two COFs were conducted to optimize the lattice parameters iteratively until the R_{wp} value converges.

Section 2. Synthetic Procedures

Section 2.1 Synthesis of Monomers

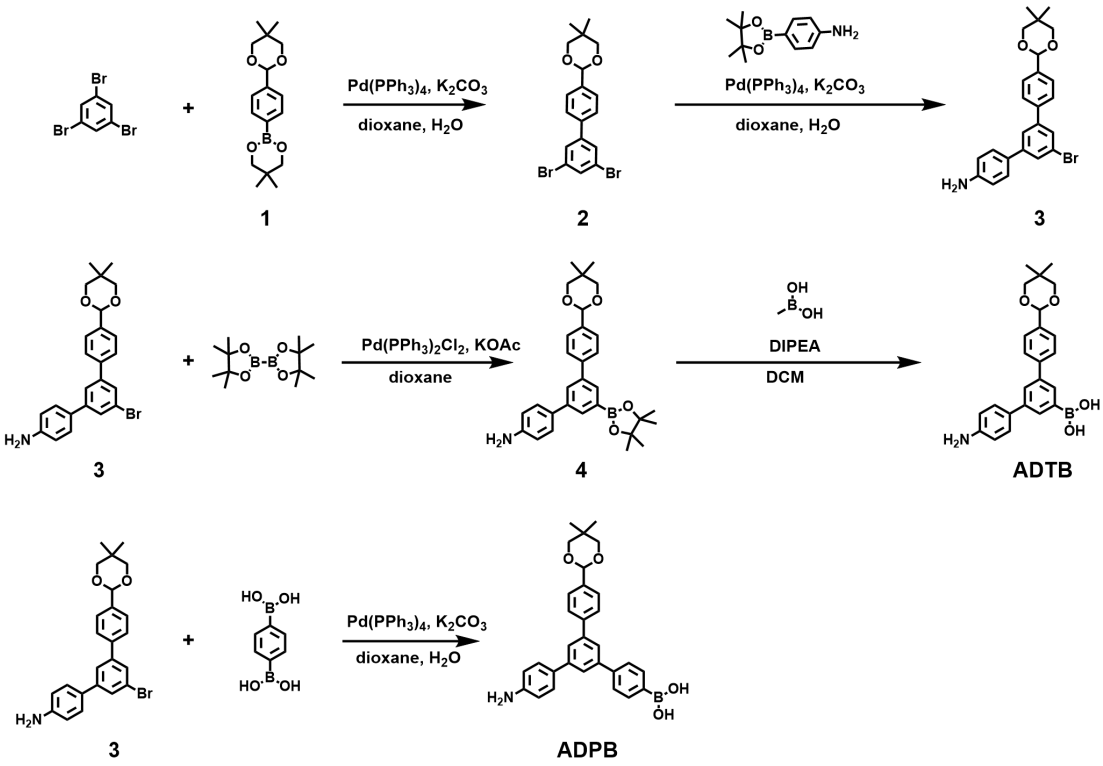

Supplementary Scheme 1. Synthetic route of **ADTB** and **ADPB**.

2-(4-(5,5-dimethyl-1,3-dioxan-2-yl)-phenyl)-5,5-dimethyl-1,3,2-dioxaborinane (1): The synthetic procedure was according to the literature[1].

5-(3',5'-dibromo-[1,1'-biphenyl]-4-yl)-2,2-dimethyl-1,3-dioxane (2): 1 (2.74 g, 9.00 mmol), 1,3,5-tribromobenzene (3.14 g, 10.00 mmol) and K_2CO_3 (5.53 g, 40.00 mmol) were mixed with $Pd(PPh_3)_4$ (1.15 g, 1.00 mmol) in a 250 mL two neck flask. Then, 1,4-dioxane (100 mL) and H_2O (20 mL) were added under argon and refluxed at 80 ℃. After 4 hours, the mixture was diluted with water and extracted with DCM. The organic layers were combined and dried over anhydrous $MgSO_4$, filtered and concentrated under reduced pressure. The residue was purified by silica gel column chromatography (EA : PE = 10:1) to obtain white solid 2. Yield: 1.42 g, 37%. ^{1}H NMR (400 MHz, $CDCl_3$) δ (ppm) 7.63 (s, 3H), 7.58 (d, 2H), 7.54 (d, 2H), 5.44 (s, 1H), 3.78 (d, 2H), 3.69 (d, 2H), 1.31 (s, 3H), 0.82 (s, 3H). ^{13}C NMR (100 MHz, $CDCl_3$) δ (ppm) 144.49, 138.84, 133.06, 132.73, 129.04, 127.11, 126.92, 123.32, 101.26, 30.35, 23.14, 21.98. MS (HR-ESI): m/z Calcd. $C_{18}H_{18}Br_2O_2$: 425.9653, found $[M - H]^-$: 424.8762.

5'-bromo-4''-(2,2-dimethyl-1,3-dioxan-5-yl)-[1,1':3',1''-terphenyl]-4-amine (3): 2 (1.00 g, 2.35 mmol), 4-aminophenylboronicacidpinacolester (0.51 g, 2.35 mmol), K_2CO_3 (1.33 g, 9.60 mmol) were mixed with $Pd(PPh_3)_4$ (0.27 g, 0.24 mmol) in a 100 mL two neck flask. Then, 1,4-dioxane (50 mL) and H_2O (10 mL) were added under argon and refluxed at 100 ºC. After 8 hours, the mixture was diluted with water and extracted with DCM. The organic layers were combined and dried over anhydrous $MgSO_4$, filtered and concentrated under reduced pressure. The residue was purified by silica gel column chromatography (EA : PE = 3:1) to obtain yellow solid 3. Yield: 0.54 g, 53%. ^{1}H NMR (400 MHz, $CDCl_3$) δ (ppm) 7.64 (m, 1H), 7.62 (m, 1H), 7.41-7.43 (m, 5H), 6.75-6.77 (d, 2H), 5.45 (d, 1H) ,3.78-3.69 (m, 6H), 1.32 (s, 1H), 0.82 (s, 1H). ^{13}C NMR (100 MHz, $CDCl_3$) δ (ppm) 146.32, 143.64, 143.26, 140.54, 138.21, 130.02, 128.29, 128.19, 127.93, 127.22, 126.76, 124.10, 123.24, 115.55, 101.45, 30.36, 23.15, 21.99. MS (HR-ESI): m/z Calcd. $C_{24}H_{24}BrNO_2$: 437.0990, found $[M + H]^+$: 438.1132.

4''-(2,2-dimethyl-1,3-dioxan-5-yl)-5'-(4,4,5,5-tetramethyl-1,3,2-dioxaborolan-2-yl) -[1,1':3',1''-terphenyl]-4-amine (4): 3 (2.00 g, 5.00 mmol), bis(pinacolato)diboron (4.64 g, 18.30 mmol), KOAc (4.00 g, 36.60 mmol) and $Pd(PPh_3)_2Cl_2$ (0.32 g, 0.46 mmol) were dissolved in 100 mL 1,4-dioxane under nitrogen and refluxed at 100 °C. After 24 hours, the mixture was diluted with water and extracted with DCM. The organic layers were combined and dried over anhydrous $MgSO_4$, filtered and concentrated under reduced pressure. The residue was purified by neutral alumina column chromatography (EA : PE = 1:1) to obtain white solid 4. Yield: 1.87 g, 85%. ^{1}H NMR (400 MHz, $CDCl_3$) δ (ppm) 7.95-7.97 (d, 1.95 H), 7.83 (m, 0.97 H), 7.68-7.70 (d, 2.04 H), 7.57-7.59 (d, 2.08 H), 7.51-7.53 (d, 2.06 H), 6.83-6.85 (d, 2.02 H), 5.45 (s, 1 H), 3.70-3.79 (m, 4 H), 1.37 (s, 12.11 H), 0.82 (s, 3H) 7.51-7.53 (d, 2.06 H),. ^{13}C NMR (100 MHz, $CDCl_3$) δ (ppm) 145.77, 141.82, 141.11, 140.74, 137.51, 131.97, 131.48, 128.32, 128.27, 127.32, 126.52, 115.51, 101.65, 83.95, 83.57, 30.34, 25.09, 24.95, 24.63, 24.17, 23.15, 22.00. MS (HR-ESI): m/z Calcd. $C_{30}H_{36}BNO_4$: 485.2737, found $[M]^+$: 485.3127.

(4-amino-4''-(2,2-dimethyl-1,3-dioxan-5-yl)-[1,1':3',1''-terphenyl]-5'-yl) boronic acid (ADTB): 4 (1.00 g, 2.10 mmol) and methylboronic acid (0.37 g, 6.20 mmol) were dissolved in a mixture of DCM (19 mL) and DIPEA (1 mL). And then, the mixture was

stirred under air at room temperature. After 48 hours, the mixture was concentrated under reduced pressure and purified by silica gel column chromatography (EA : PE = 1:1) to obtain white solid ADTB. Yield: 0.41 g, 48%. ^{1}H NMR (400 MHz, $CDCl_3$) δ (ppm) 8.26 (s, 1.02 H), 7.82 (s, 1.62 H), 7.45-7.67 (m, 6.54 H), 6.75 (s, 2.02 H), 5.43 (s, 1 H), 3.67-3.78 (m, 6 H), 1.31 (s, 3H), 0.80 (s, 3 H). ^{13}C NMR (100 MHz, $CDCl_3$) δ (ppm) 144.79, 142.48, 142.03, 140.42, 137.21, 137.04, 133.38, 131.98, 131.15, 127.98, 127.89, 127.21, 126.68, 117.00, 116.19, 101.69, 30.20, 23.10, 21.83.MS (HR-ESI), m/z Calcd. $C_{24}H_{26}BNO_4$: 403.1955, found $[M + H]^+$:404.2104.

(4''-amino-5'-(4-(2,2-dimethyl-1,3-dioxan-5-yl)phenyl)-1,2-dihydro-[1,1':3',1''-terphenyl]-4-yl)boronic acid (ADPB): 3 (1.00 g, 2.28 mmol), 1,4-phenylenebisboronic acid (0.38 g, 2.28 mmol), K_2CO_3 (5.60 g, 40.00 mmol) were mixed with $Pd(PPh_3)_4$ (0.14 g, 0.12 mmol) in a 100 mL two neck flask. Then, 1,4-dioxane (50 mL) and H_2O (10 mL) were added under air and refluxed at 100 °C. After 4 hours, the mixture was diluted with water and extracted with DCM. The organic layers were combined and dried over anhydrous $MgSO_4$, filtered and concentrated under reduced pressure. The residue was purified by silica gel column chromatography (EA : PE = 1:1) to obtain white solid ADPB. Yield: 0.63 g, 57%. ^{1}H NMR (400 MHz, $CDCl_3$) δ (ppm) 7.78-7.79 (m, 3.43 H), 7.71-7.75 (m, 4.63 H), 7.61-7.63 (m, 2.39 H), 7.52-7.55 (m, 2.39 H), 6.80-6.82 (m, 2.26 H), 5.48 (s, 1 H), 3.71-3.79 (m, 6 H), 1.33 (s, 3 H), 0.83 (s, 3H). ^{13}C NMR (100 MHz, $CDCl_3$) δ (ppm) 146.15, 142.35, 142.00, 141.88, 141.76, 140.45, 137.73, 131.36, 128.86, 128.28, 127.79, 127.35, 126.63, 124.60, 124.52, 124.19, 115.45, 101.56, 30.32, 23.11, 21.96. MS (HR-ESI), m/z Calcd. $C_{30}H_{30}BNO_4$: 479.2268, found $[M + H]^+$: 480.2396.

Section 2.2 Synthesis of COFs

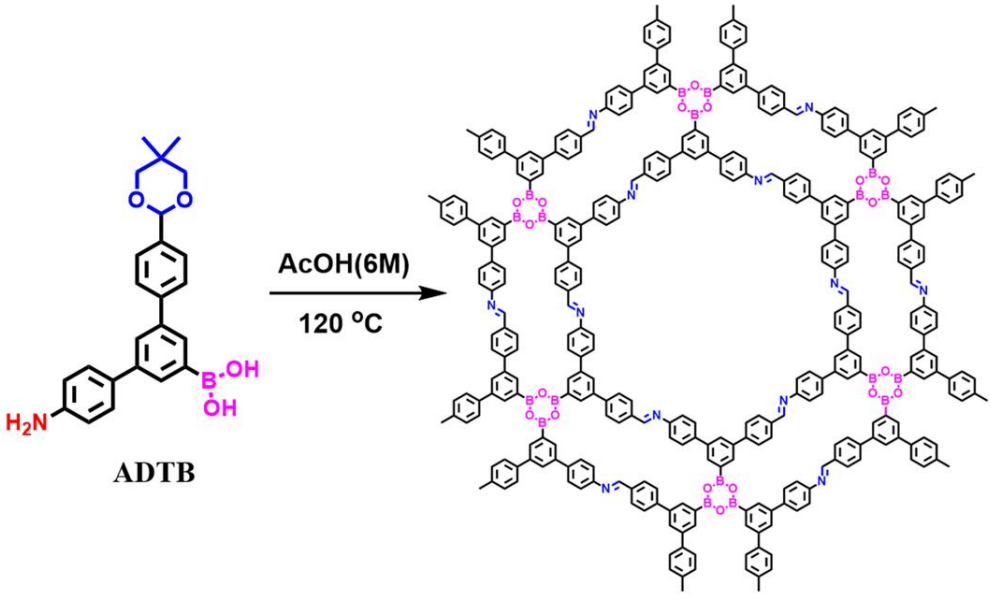

Supplementary Scheme 2. Synthetic route of **ADTB-COF**.

ADTB-COFs: A 10 mL Pyrex tube was charged with ADTB (22.00 mg, 0.054 mmol), and 1 mL toluene was added (Experiments on different solvent systems were carried out and shown in section 4). After the mixture was sonicated for 1 min, 0.20 mL of acetic acid (6 M) was added. The mixture was sonicated for another 1 min and further degassed by three freeze-pump-thaw cycles, purged with N_2 and then heated at 120 °C for 3 days. After cooling, the precipitate was collected by filtration and washed by THF, ethyl alcohol and acetone. The collected sample was dried under vacuum for 24 h to afford ADTB-COFs (10.60 mg, 69%) as yellow powder. Anal. Calcd. for $C_{19}H_{12}BNO$: C, 81.18%; H, 4.30%; N, 4.98%. Found: C, 78.10%; H, 4.42%; N, 4.59%.

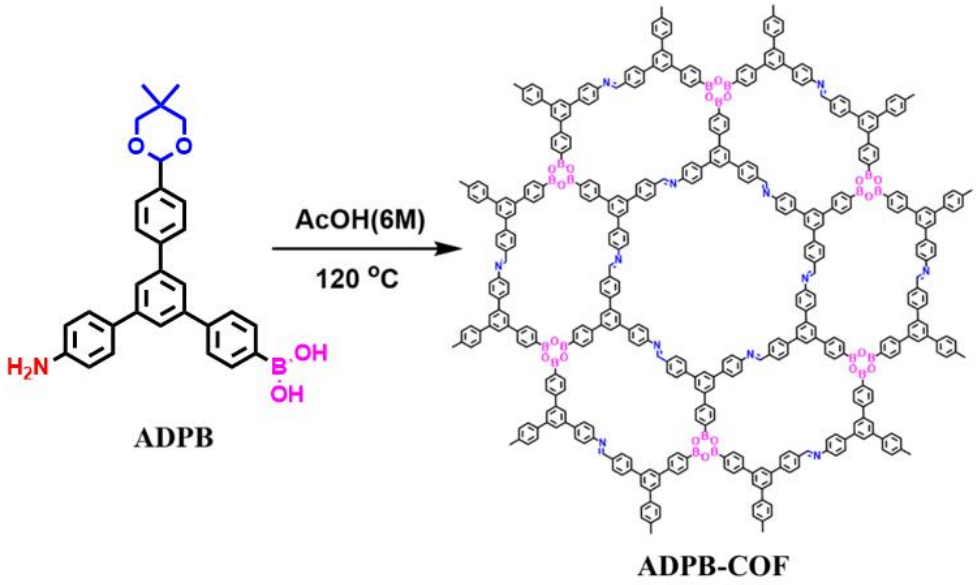

Supplementary Scheme 3. Synthetic route of **ADPB-COF**.

ADPB-COFs: A 10 mL Pyrex tube was charged with ADPB (26.00 mg, 0.056 mmol), then 1 mL *n*-BuOH and 1 mL *o*-DCB were added (Experiments on different solvent systems were carried out and shown in section 4). After the mixture was sonicated for 2 min, 0.20 mL of acetic acid (6 M) was added. The mixture was sonicated for another 1 min and further degassed by three freeze-pump-thaw cycles, purged with N_2 and then heated at 120 °C for 3 days. After cooling, the precipitate was collected by filtration and washed by THF, ethyl alcohol and acetone. The collected sample was dried under vacuum for 24 h to afford ADPB-COFs (16.40 mg, 85%) as a yellow-green powder. Anal. Calcd. for $C_{25}H_{16}BNO$: C, 84.06%; H, 4.51%; N, 3.92%. Found: C, 83.54%; H, 5.18%; N, 4.01%.

Section 3. NMR and Mass Spectra

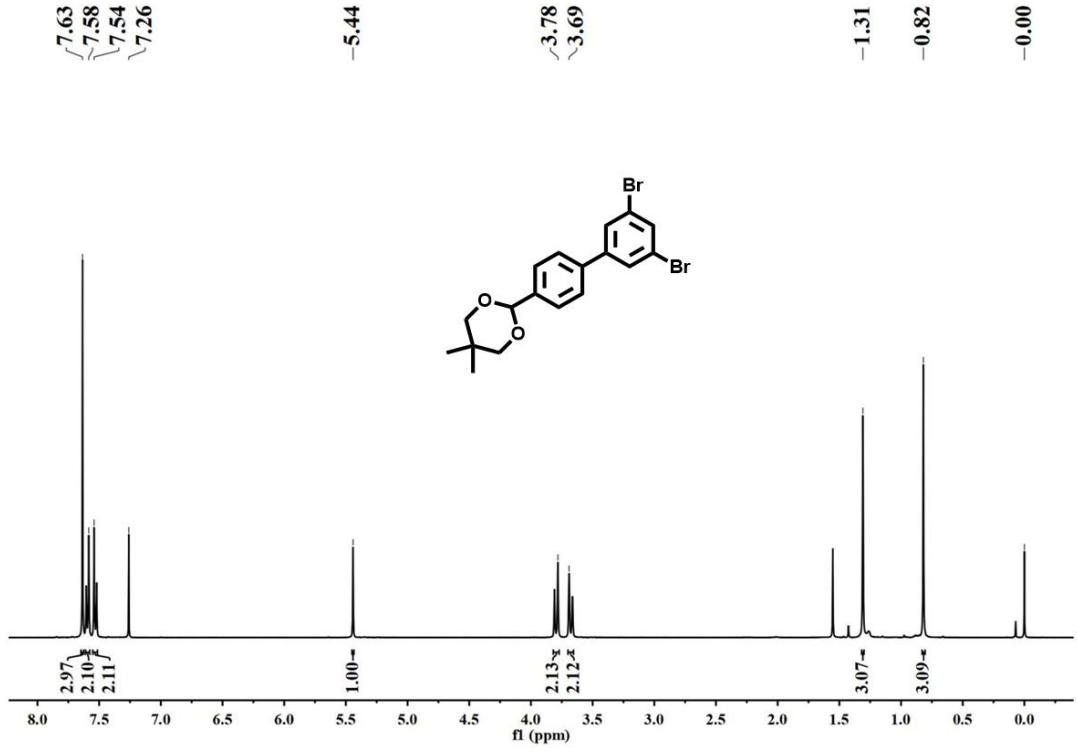

Supplementary Figure 1. ^{1}H NMR spectrum of compound **2** in $CDCl_3$ (400 MHz).

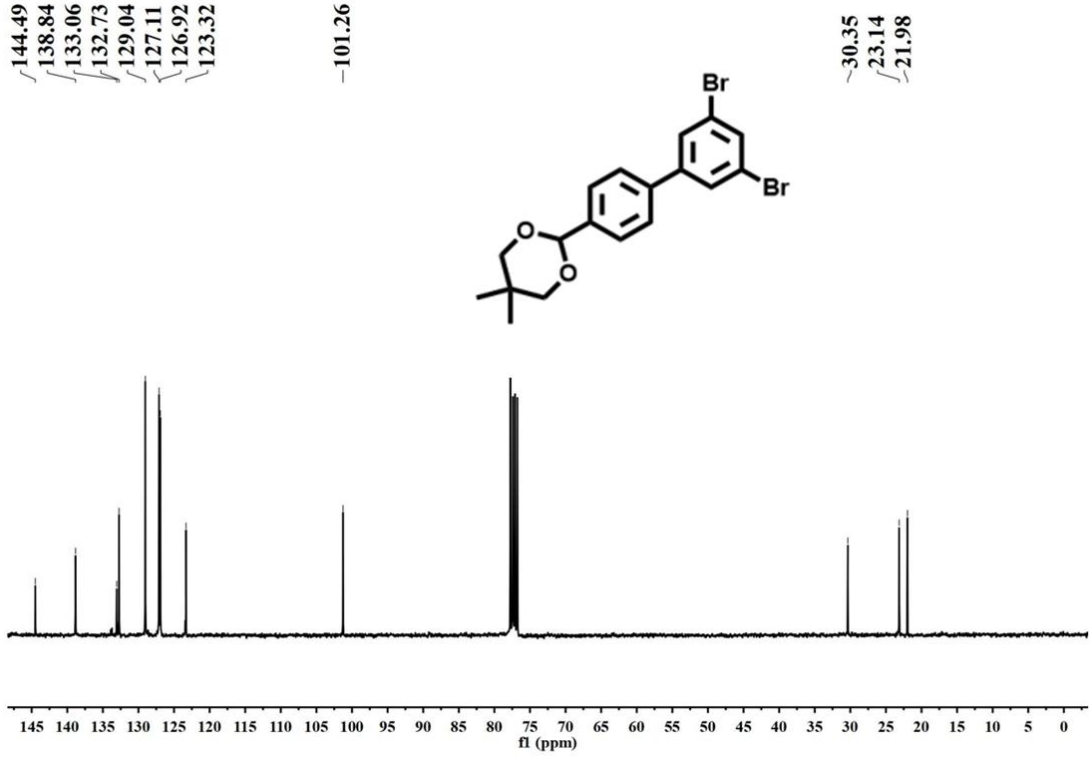

Supplementary Figure 2. ^{13}C NMR spectrum of compound **2** in $CDCl_3$ (100 MHz).

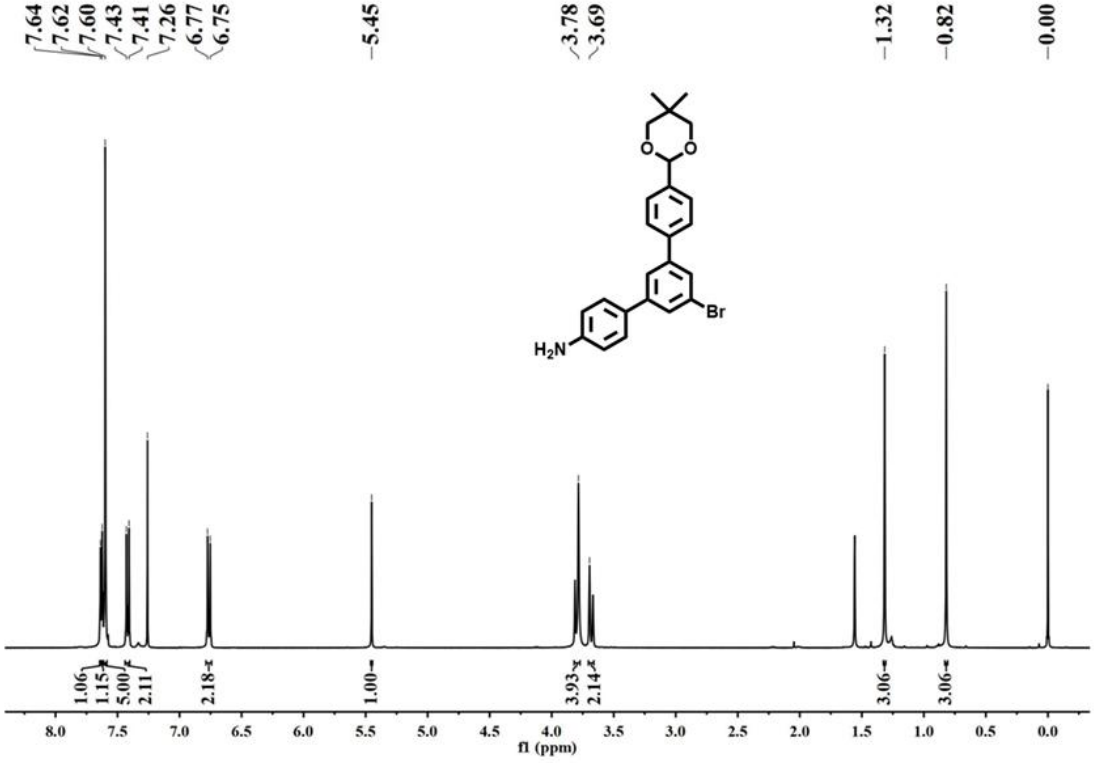

193

194 **Supplementary Figure 3.** ^{1}H NMR spectrum of compound **3** in $CDCl_3$ (400 MHz).

195

196

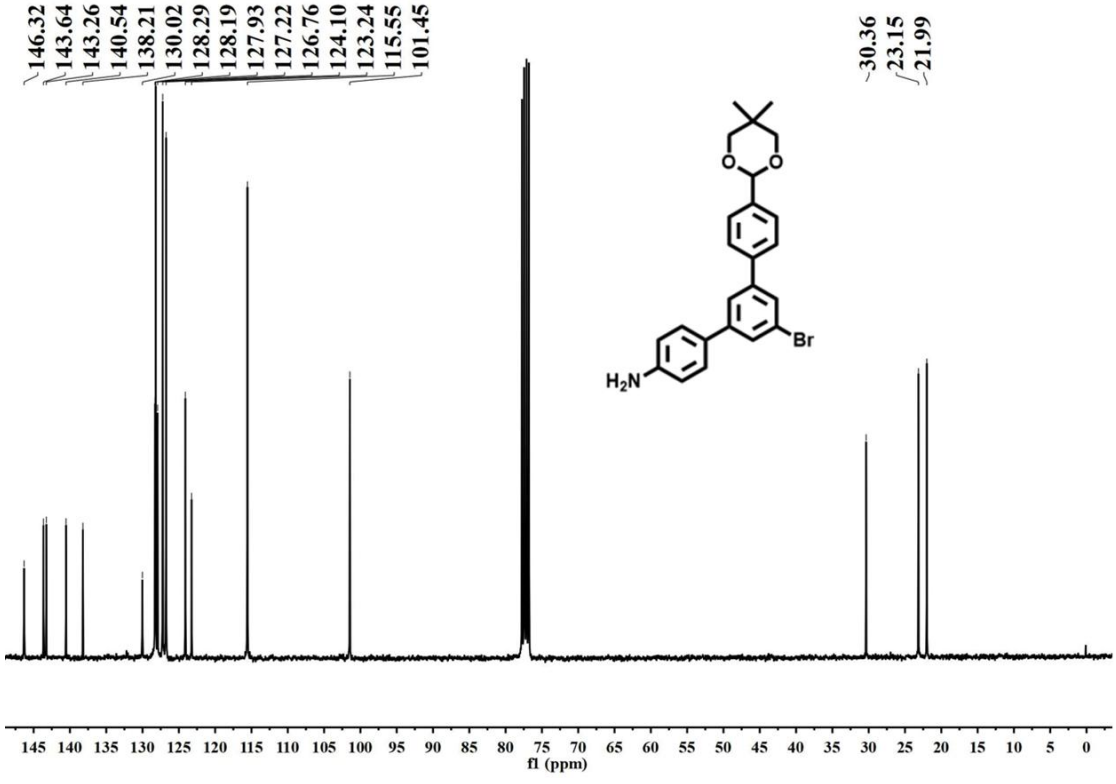

197

198 **Supplementary Figure 4.** ^{13}C NMR spectrum of compound **3** in $CDCl_3$ (100 MHz).

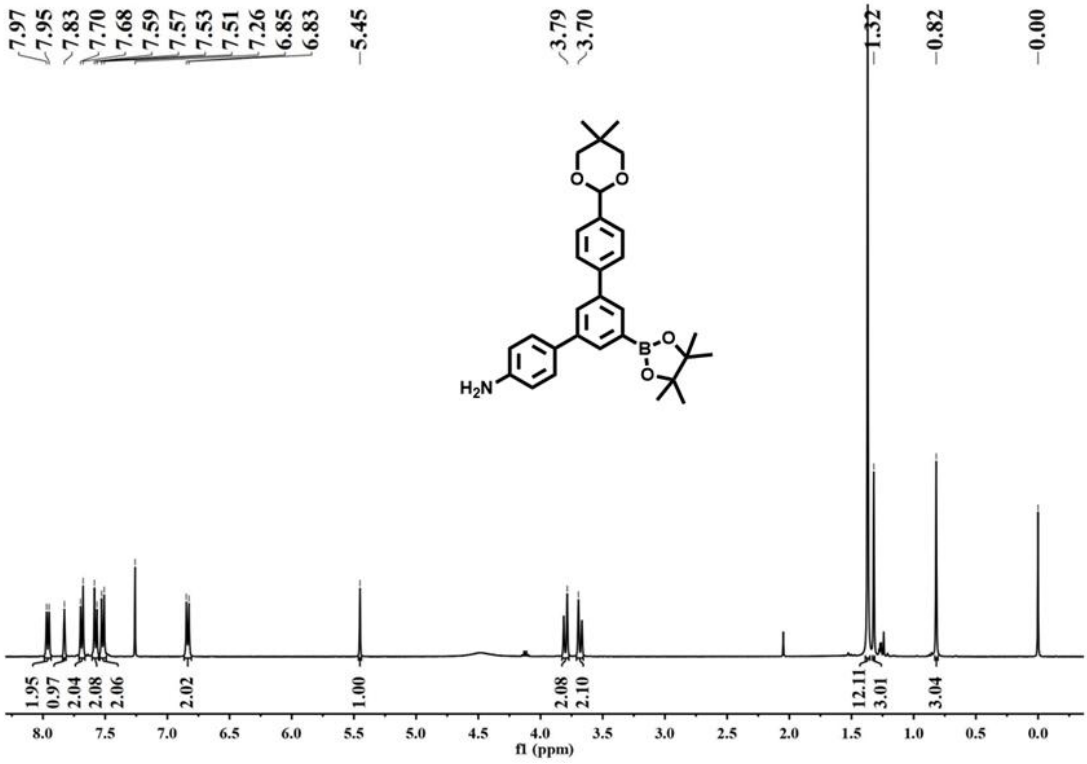

Supplementary Figure 5. ^{1}H NMR spectrum of compound **4** in $CDCl_3$ (400 MHz).

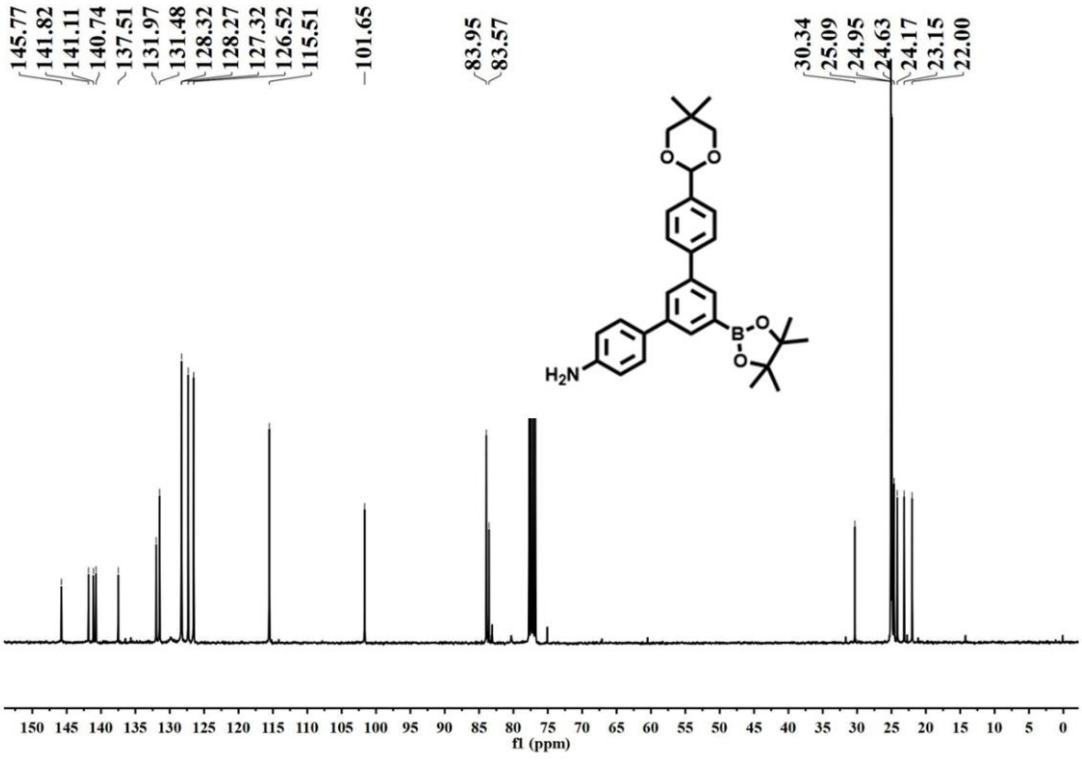

Supplementary Figure 6. ^{13}C NMR spectrum of compound **4** in $CDCl_3$ (100 MHz).

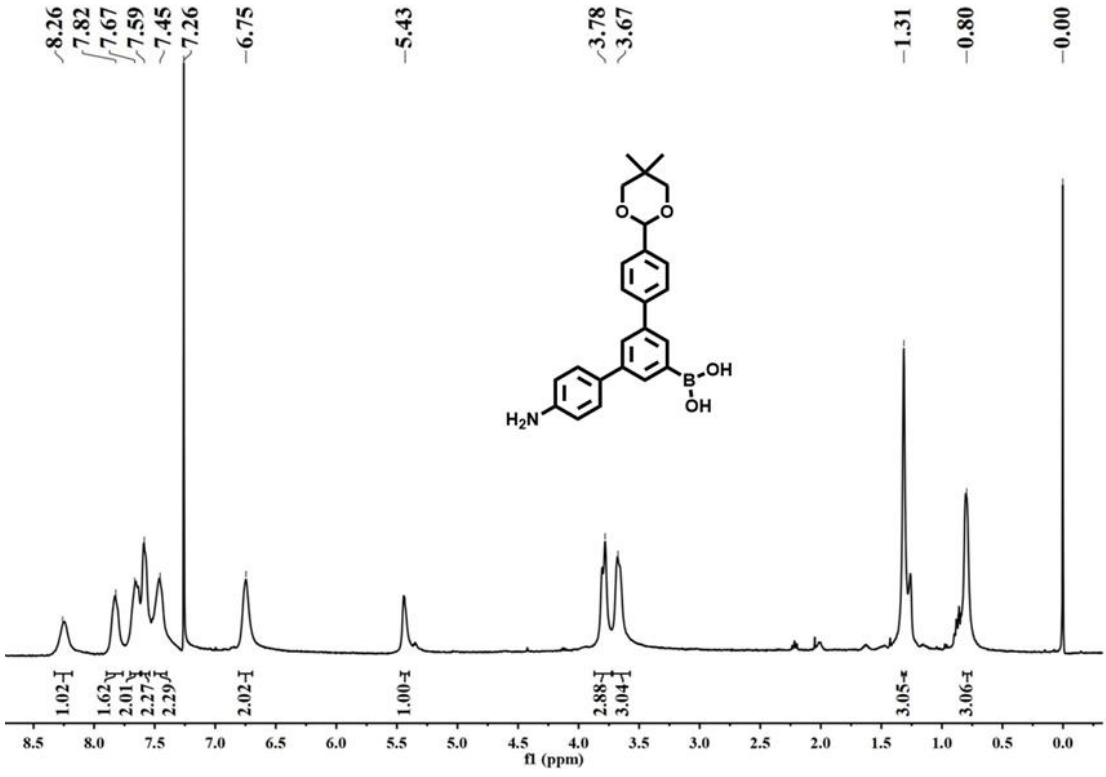

205

206 **Supplementary Figure 7.** ^{1}H NMR spectrum of compound **ADTB** in $CDCl_3$ (400

207 MHz).

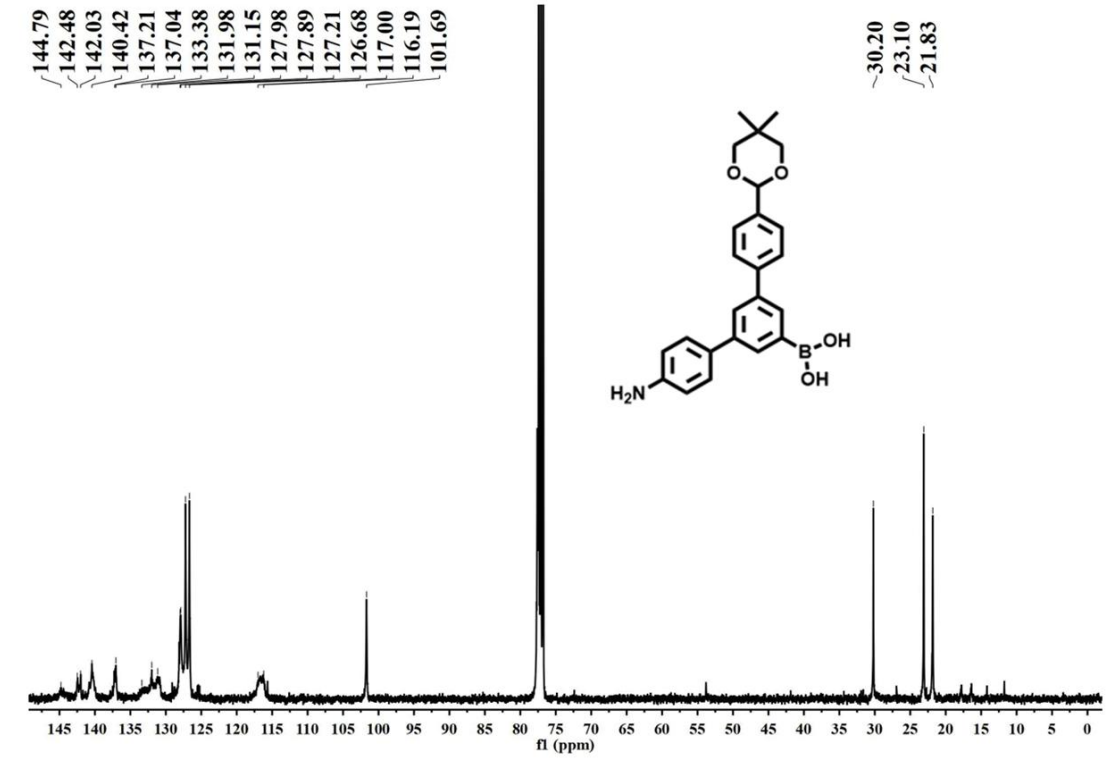

208

209 **Supplementary Figure 8.** ^{13}C NMR spectrum of compound **ADTB** in $CDCl_3$ (100

210 MHz).

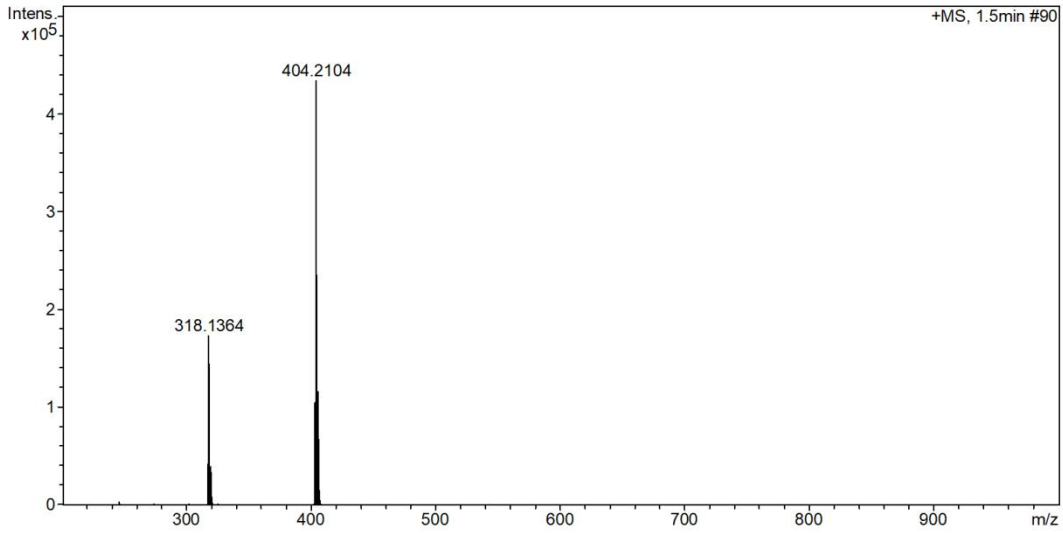

211

212 **Supplementary Figure 9.** High resolution mass spectrum of compound **ADTB**.

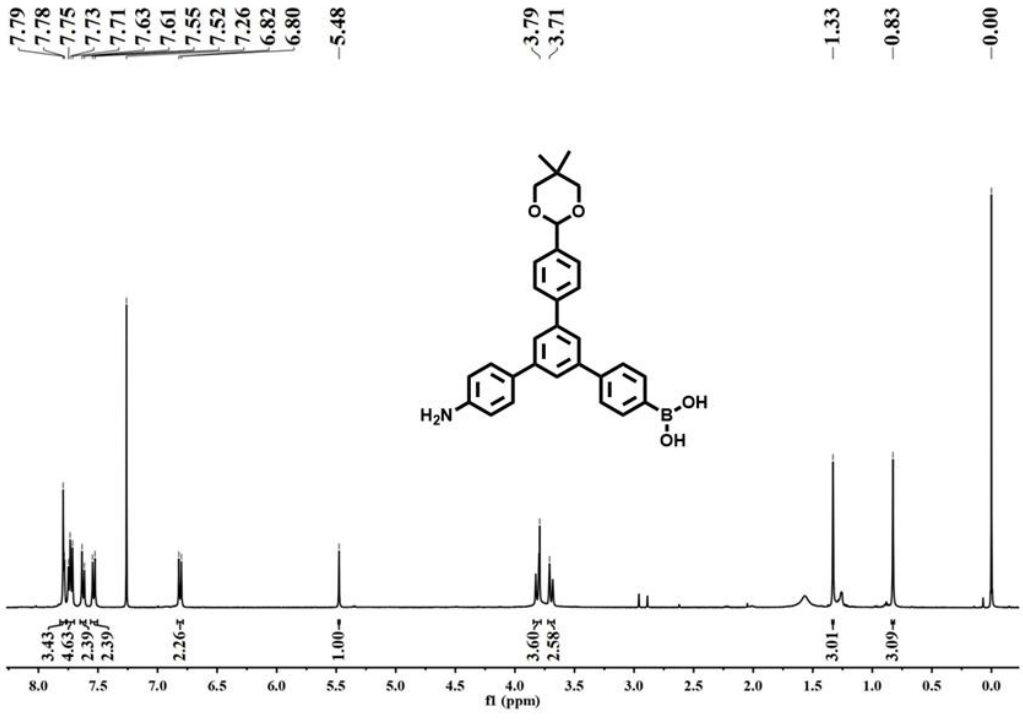

213

214 **Supplementary Figure 10.** ^{1}H NMR spectrum of compound **ADPB** in $CDCl_3$ (400

215 MHz).

216

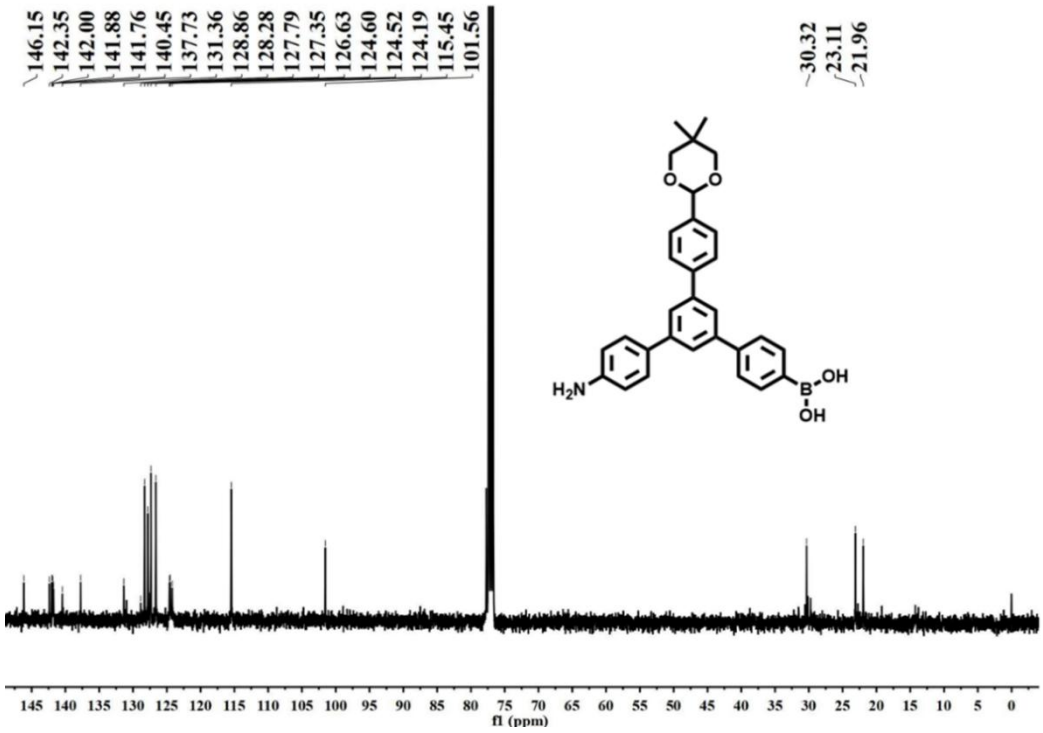

Supplementary Figure 11. ^{13}C NMR spectrum of compound **ADPB** in $CDCl_3$ (100 MHz).

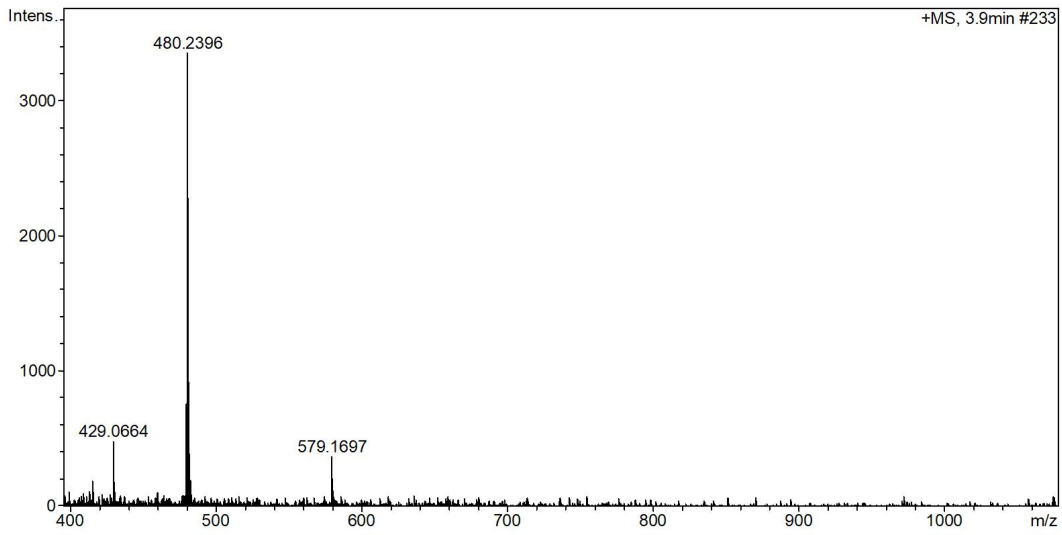

Supplementary Figure 12. High resolution mass of compound **ADPB**.

Section 4. Experiments in different solvent systems

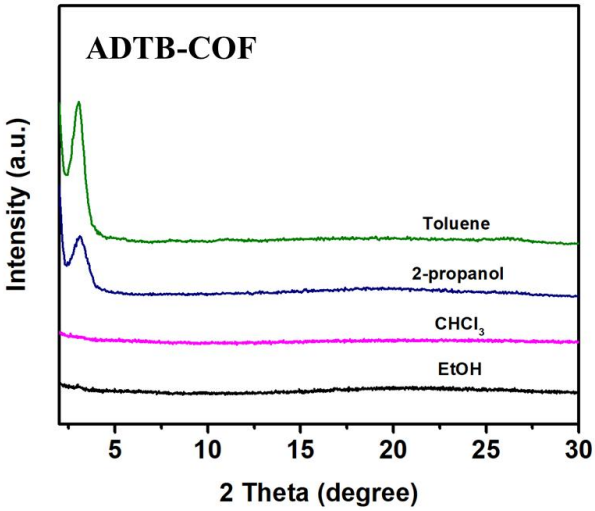

Supplementary Figure 13. PXRD of ADTB-COF in different solvents (The solid powders can only be obtained in a few solvent systems).

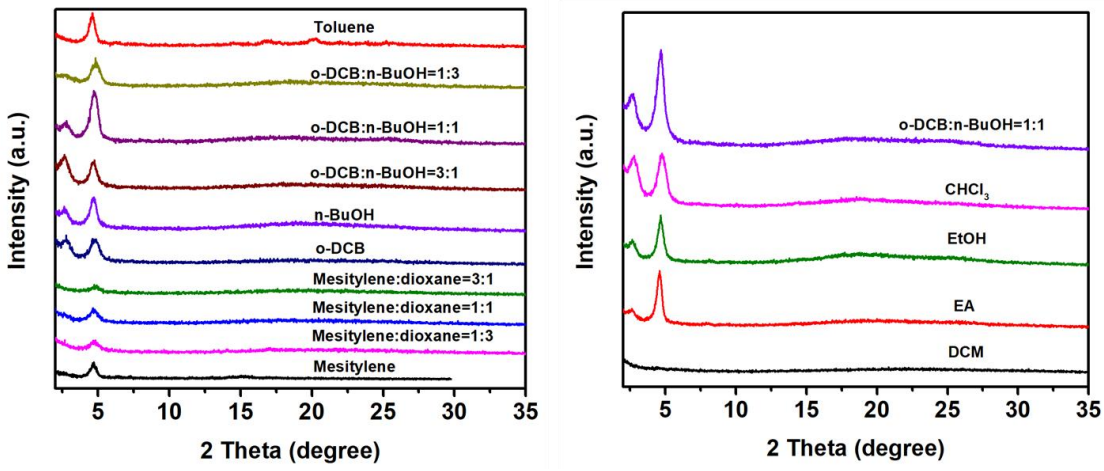

Supplementary Figure 14. PXRD of ADPB-COF in different solvents (The solid powders can be obtained in various solvent systems).

Section 5. FT-IR Spectra

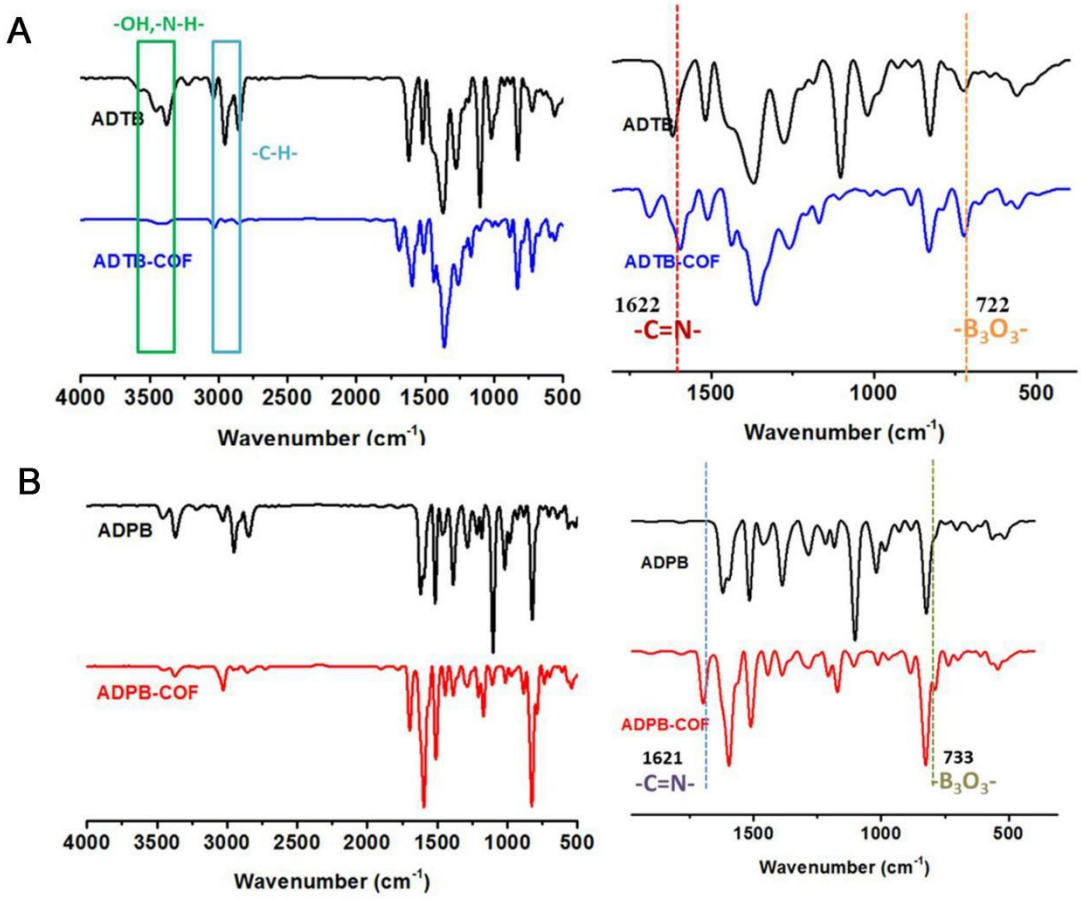

Supplementary Figure 15. FT-IR spectra comparison of ADTB, ADPB, ADTB-COF and ADPB-COF.

Section 6. Solid-State ^{13}C CP/MAS NMR spectrum

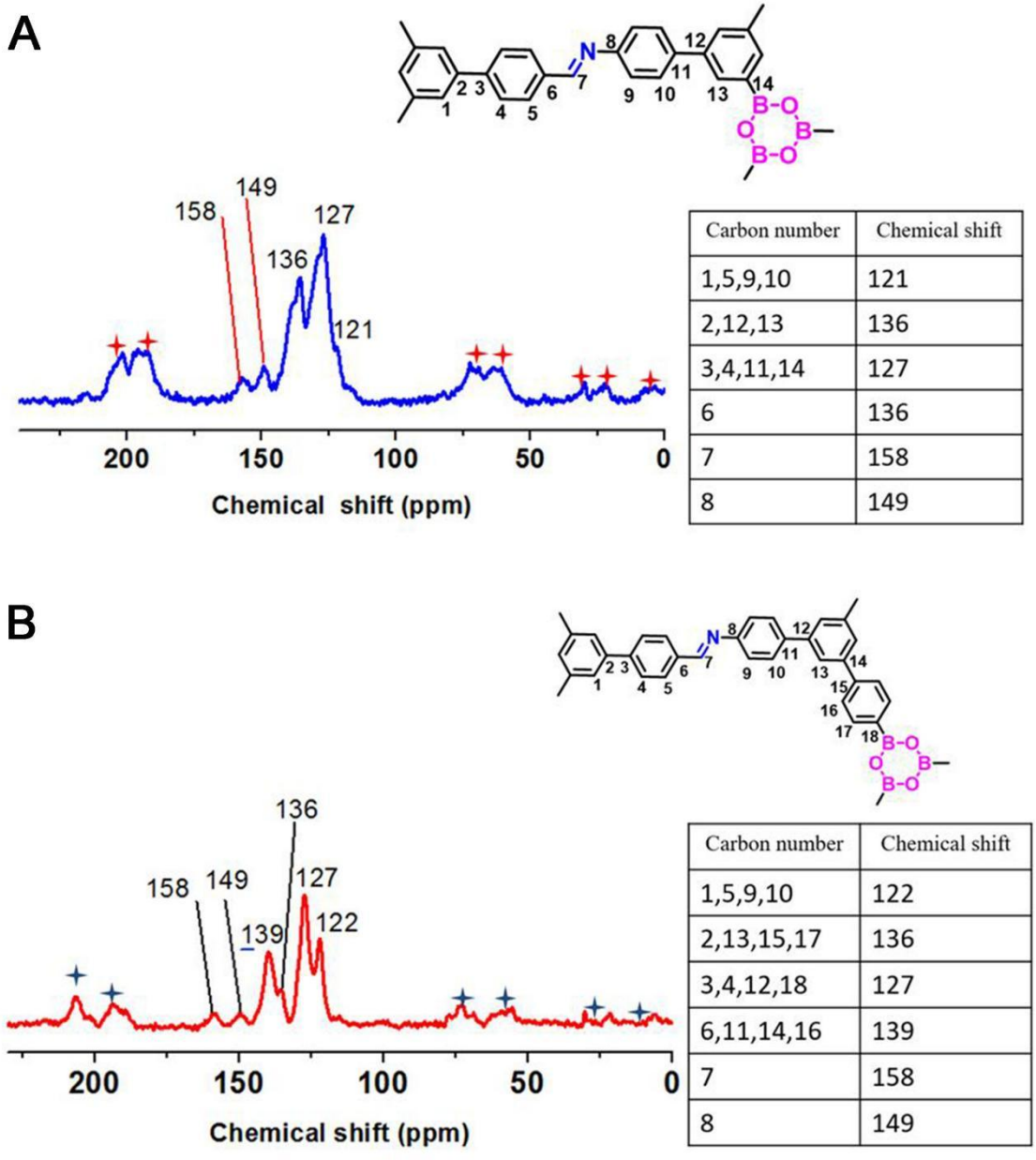

Carbon number	Chemical shift
1,5,9,10	121
2,12,13	136
3,4,11,14	127
6	136
7	158
8	149

Carbon number	Chemical shift
1,5,9,10	122
2,13,15,17	136
3,4,12,18	127
6,11,14,16	139
7	158
8	149

Supplementary Figure 16. Solid-state ^{13}C CP/MAS NMR spectrum of (A) ADTB-COF and (B) ADPB-COF. Signals with stars are sidebands.

Section 7. PXRD Patterns and Structural Analysis

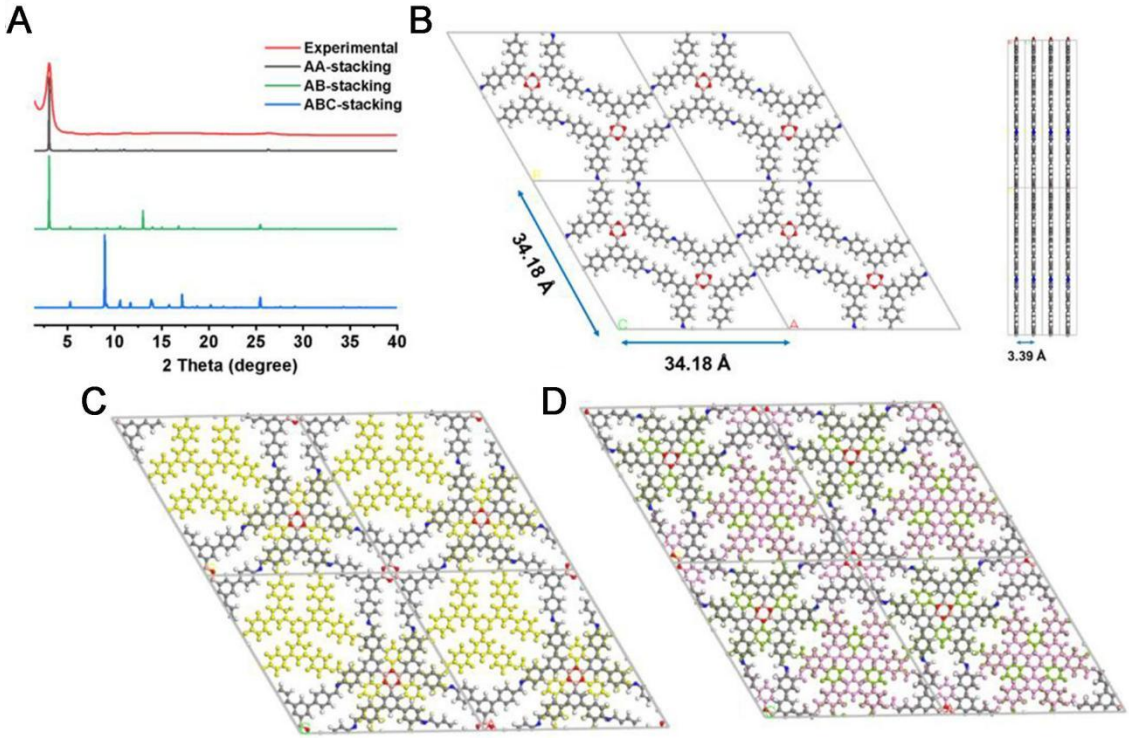

Supplementary Figure 17. (A) Experimental (red), AA stacking, AB stacking and ABC stacking XRD of ADTB-COF. (B) Top-view and side-view for AA stacking model of ADTB-COF. Top-view for (C) AB stacking and (D) ABC stacking model of ADTB-COF.

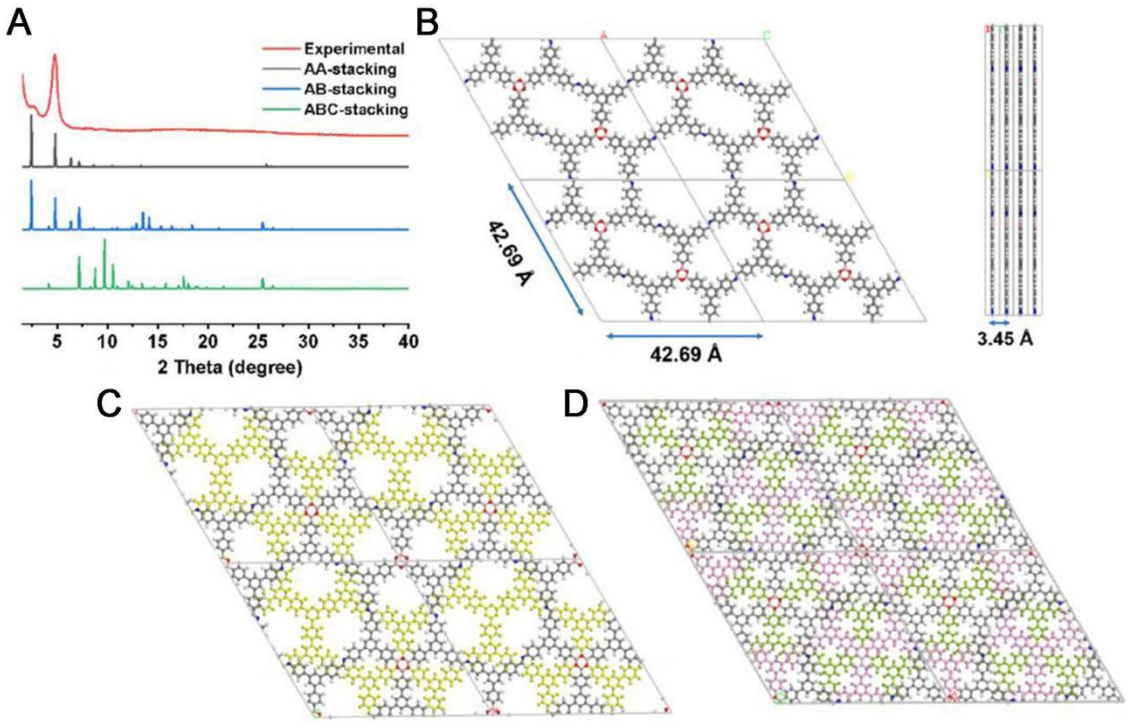

Supplementary Figure 18. (A) Experimental (red), AA stacking, AB stacking and ABC stacking XRD of ADPB-COF. (B) Top-view and side-view for AA stacking model of ADPB-COF. Top-view for (C) AB stacking and (D) ABC stacking model of ADPB-COF.

Section 8. Thermogravimetric Analysis

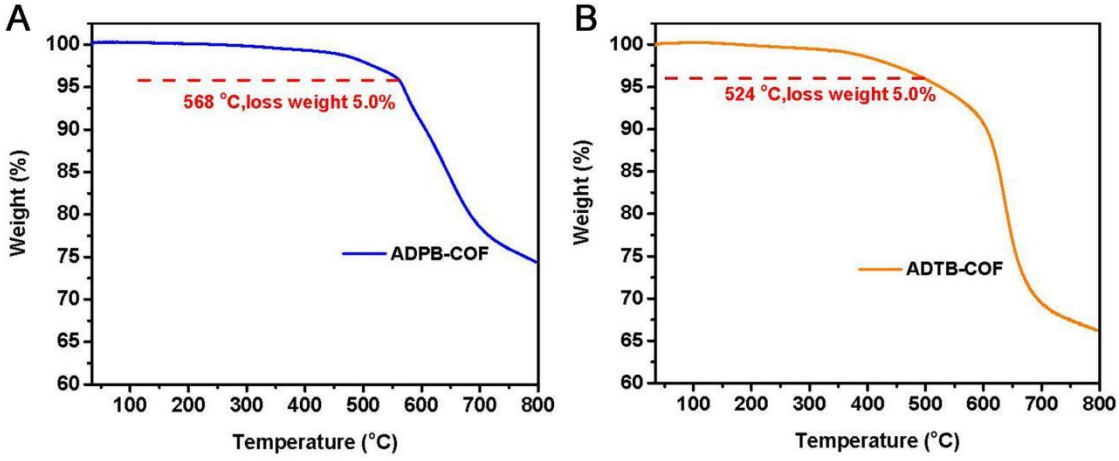

Supplementary Figure 19. Thermogravimetric analysis profiles of (A) ADPB-COF and (B) ADTB-COF.

Section 9. Stability of Water Resistance

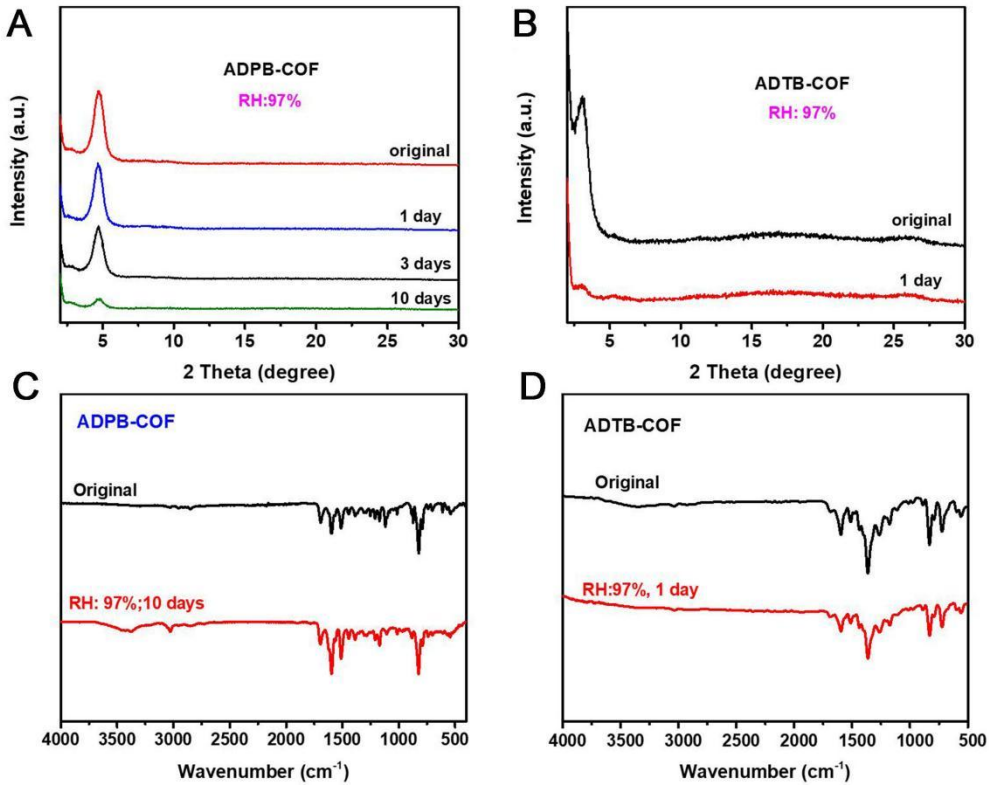

Supplementary Figure 20. Comparison of changes in PXRD patterns of ADTB-COF (A) and ADPB-COF (B) placed in an environment with 97% relative humidity for different number of days. Comparison of changes in FT-IR spectra of **ADTB-COF** (A) and **ADPB-COF** (B) placed in an environment with 97% relative humidity for different number of days.

Section 10. Atomic Coordinates of ADTB-COF and ADPB-COF

Supplementary Table 1. Atomic coordinates of the AA-stacking mode of ADTB-COF using Forcite and DFTB$^+$ method.

Space group: *P*6/*M*			
***a* = *b* = 34.18 Å, and *c* = 3.39 Å**			
***α* = *β* = 90, and *γ* = 120°**			
	X	**Y**	**Z**
C1	-1.52909	-3.7564	0.5
C2	-1.508	-3.78321	0.5
C3	-1.46035	-3.76013	0.5
C4	-1.43491	-3.71316	0.5
C5	-1.45649	-3.68777	0.5
C6	-1.50402	-3.7084	0.5
C7	-1.52675	-3.6798	0.5
C8	-1.53496	-3.83462	0.5
C9	-1.50094	-3.6319	0.5
C10	-1.52135	-3.60543	0.5
C11	-1.56826	-3.62522	0.5
C12	-1.59477	-3.6724	0.5
C13	-1.57444	-3.69929	0.5
C14	-1.58285	-3.85906	0.5
C15	-1.60703	-3.9064	0.5
C16	-1.5847	-3.93123	0.5
C17	-1.53728	-3.90762	0.5
C18	-1.5131	-3.8606	0.5
C19	-1.00747	-3.41208	0.5
B20	-1.31109	-3.69304	0.5
N21	-1.02009	-3.63136	0.5
O22	-1.28339	-3.64381	0.5
H23	-1.56503	-3.7729	0.5
H24	-1.44172	-3.77772	0.5
H25	-1.43501	-3.65176	0.5
H26	-1.46468	-3.61317	0.5

H27	-1.50006	-3.56897	0.5
H28	-1.63127	-3.68862	0.5
H29	-1.59717	-3.73521	0.5
H30	-1.60284	-3.84277	0.5
H31	-1.6436	-3.9239	0.5
H32	-1.51786	-3.92459	0.5
H33	-1.47705	-3.84606	0.5
H34	-0.99504	-3.43551	0.5
H32	-1.51786	-3.92459	0.5
H33	-1.47705	-3.84606	0.5
H34	-0.99504	-3.43551	0.5

273

Supplementary Table 2. Atomic coordinates of the AA-stacking mode of ADPB-COF using Forcite and DFTB$^+$ method.

Space group: *P*6/*M*			
***a* = *b* = 42.69 Å, and *c* = 3.45 Å**			
***α* = *β* = 90, and *γ* = 120°**			
	X	**Y**	**Z**
C1	4.0647	8.38924	0.5
C2	4.04288	8.35088	0.5
C3	4.06014	8.32958	0.5
C4	4.00244	8.33461	0.5
N5	4.0212	7.70244	0.5
C6	4.05887	7.71972	0.5
C7	4.07824	7.70037	0.5
C8	3.28894	8.58366	0.5
C9	3.25042	8.56547	0.5
C10	3.22971	8.52693	0.5
C11	3.24681	8.5049	0.5
C12	3.28604	8.52425	0.5
C13	3.30656	8.56279	0.5
C14	3.22426	8.46274	0.5
C15	3.18542	8.44376	0.5
C16	3.16365	8.40483	0.5
C17	3.18253	8.38467	0.5
C18	3.22151	8.40209	0.5
C19	3.24137	8.44109	0.5
C20	3.24172	8.38015	0.5
C21	3.12156	8.38572	0.5
C22	3.10301	8.40634	0.5
C23	3.09881	8.34663	0.5
C24	3.22261	8.34105	0.5
C25	3.24102	8.32006	0.5
C26	3.28155	8.39885	0.5
B27	3.62688	8.31482	0.5

O28	3.6448	8.29244	0.5
H29	4.05201	8.40637	0.5
H30	4.04382	8.29973	0.5
H31	3.99245	8.35389	0.5
H32	4.06448	7.67067	0.5
H33	3.23599	8.58097	0.5
H34	3.2003	8.51562	0.5
H35	3.30219	8.51078	0.5
H36	3.33643	8.57618	0.5
H37	3.17213	8.4596	0.5
H38	3.16679	8.35534	0.5
H39	3.27051	8.4549	0.5
H40	3.11682	8.43595	0.5
H41	3.10985	8.32828	0.5
H42	3.19298	8.32481	0.5
H43	3.22485	8.2894	0.5
H44	3.30015	8.42901	0.5

276

Section 11. Data Analysis of Specific Surface Area

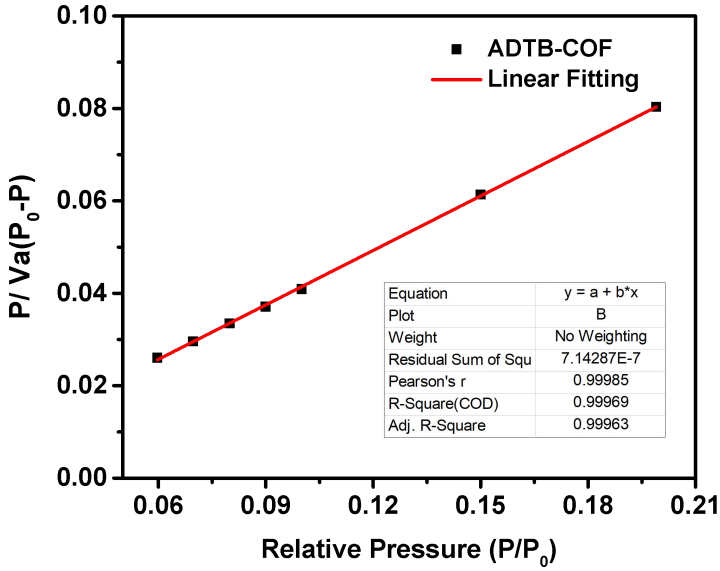

Supplementary Figure 21. BET plot for ADTB-COF.

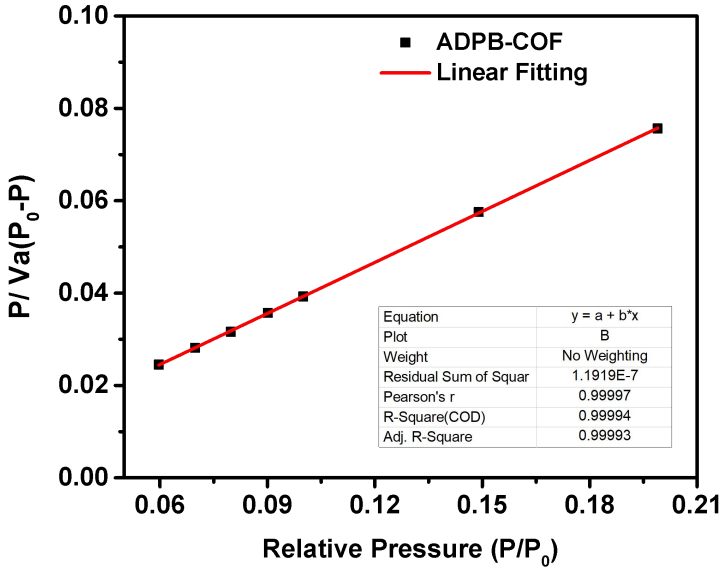

Supplementary Figure 22. BET plot for ADPB-COF.

Section 12. Gas Adsorption Properties

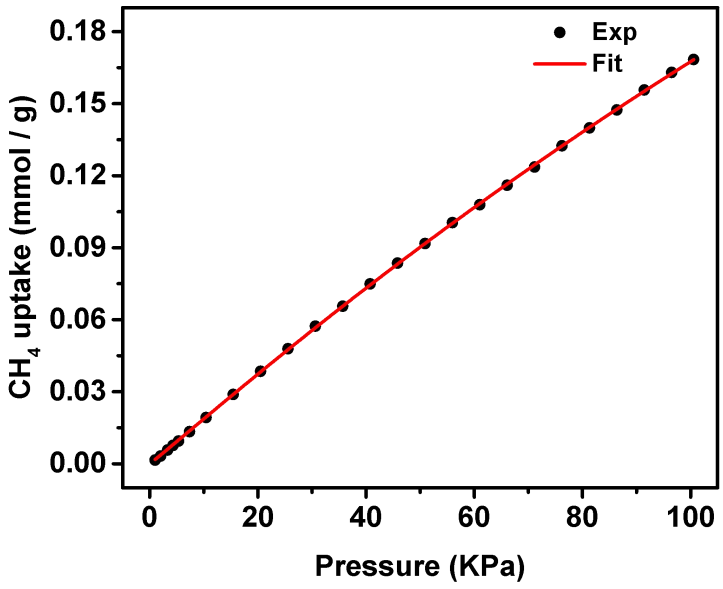

Supplementary Figure 23. Single site Langmuir-Freundlich model fitting for CH_4 adsorption of ADPB-COF.

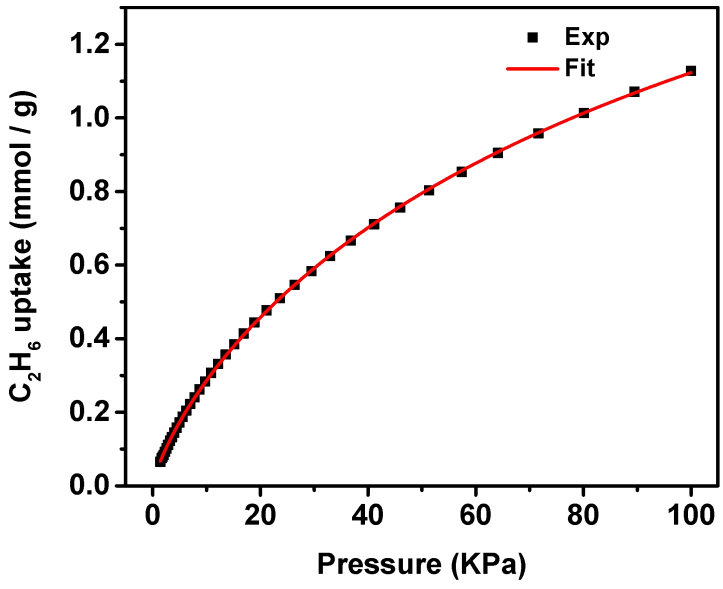

Supplementary Figure 24. Single site Langmuir-Freundlich model fitting for C_2H_6 adsorption of ADPB-COF.

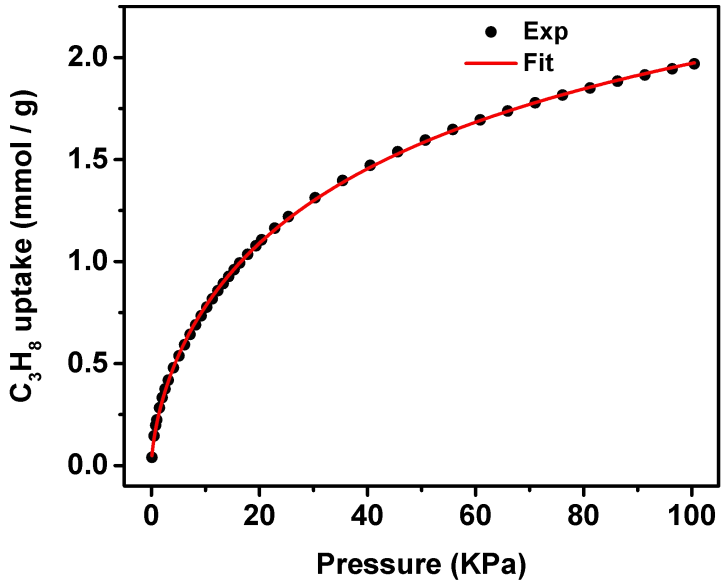

296

297 **Supplementary Figure 25.** Single site Langmuir-Freundlich model fitting for C_3H_8

298 adsorption of ADPB-COF.

299

300

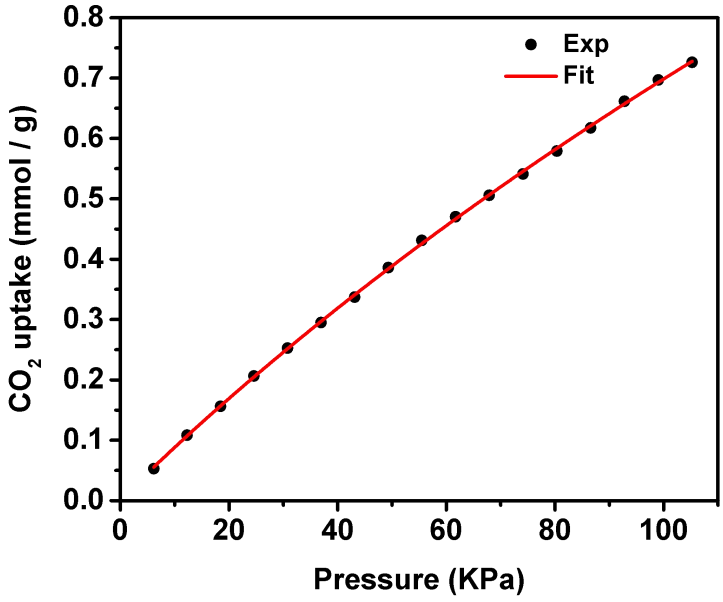

301

302 **Supplementary Figure 26.** Single site Langmuir-Freundlich model fitting for CO_2

303 adsorption of ADPB-COF.

304

Supplementary Table 3. Specific fitting parameters of the Single site Langmuir-Freundlich model for sorption isotherms[2].

Samples	Adsorbent	Model: $N = \frac{abp^c}{1+bp^c}$			
		a	b	c	R^2
ADPB-COF	CH_4	0.95342	0.00187	1.02783	0.99994
	C_2H_6	2.56761	0.02019	0.79274	0.99991
	C_3H_8	3.43732	0.06405	1.33889	0.99974
	CO_2	4.18628	0.00231	1.03138	1.00000

Supplementary Table 4. The separation ratio of C_3H_8/CH_4 (1:1) of different porous materials (298 K, 1 bar).

Materials	BET ($m^2 g^{-1}$)	C_3H_8/CH_4	Ref.
ADPB-COF	893	174	This work
Zr-OBBA	414	105.6	[3]
Zr-SDBA	739	97.5	[3]
JLU-Liu45	971	42.7	[3]
MCOF-1	874	1800	[4]
PAF-40	601	48.2	[5]
PAN-m1	904	222.8	[6]
PAN-m2	948	141.7	[6]
SMC1	1231	159.1	[7]
SMC2	1543	146	[7]
CTF-BIB-3	2088	170.5	[8]
sPI-A-B	620	204.7	[9]
sPI-M-B	618	217.4	[9]
sPI-M-H	492	82	[9]
UPC-35	1087	87.67	[10]
ZUL-C1	504	73	[11]
UPC-102-Zr	2182.5	42.5	[12]
UPC-101-Al	2083.8	37.2	[12]
JLU-Liu5	707	107.8	[13]

Section 13. REFERENCES

1. Z. Zhao, J. Zhao, S. Zhang, et al. Topology modulation of 2D covalent organic frameworks via a “two-in-one” strategy. *Nanoscale* 2021;13:19385-19390. [PMID: 34812818 DOI: 10.1039/d1nr05758h]

2. C. Jia, R. R. Liang, S. X. Gan, S. Y. Jiang, Q. Y. Qi and X. Zhao. Boosting Hydrostability and Carbon Dioxide Capture of Boroxine-Linked Covalent Organic Frameworks by One-Pot Oligoamine Modification. *Chem Eur J* 2023;29:e202300186. [PMID: 36859630 DOI: 10.1002/chem.202300186]

3. J. Gu, X. Sun, L. Kan, J. Qiao, G. Li and Y. Liu. Structural Regulation and Light Hydrocarbon Adsorption/Separation of Three Zirconium–Organic Frameworks Based on Different V-Shaped Ligands. *ACS Appl Mater Inter* 2021;13:41680-41687. [PMID: 34433263 DOI: 10.1021/acsami.1c11224]

4. H. Ma, H. Ren, S. Meng, et al. A 3D microporous covalent organic framework with exceedingly high C_3H_8/CH_4 and C_2 hydrocarbon/CH_4 selectivity. *Chem Commun* 2013;49:9773-9775. [PMID: 24022638 DOI: 10.1039/c3cc45217d]

5. S. Meng, H. Ma, L. Jiang, H. Ren and G. Zhu. A facile approach to prepare porphyrinic porous aromatic frameworks for small hydrocarbon separation. *J Mater Chem A* 2014;2:14536-14541. [DOI: 10.1039/C4TA00984C]

6. G. Li and Z. Wang. Micro- and Ultramicroporous Polyaminals for Highly Efficient Adsorption/Separation of C_1-C_3 Hydrocarbons and CO_2 in Natural Gas. *ACS Appl Mater Inter* 2020;12:24488-24497. [PMID: 32406666 DOI: 10.1021/acsami.0c04378]

7. Z. Ke, H. Xiao, Y. Wen, et al. Adsorption Property of Starch-Based Microporous Carbon Materials with High Selectivity and Uptake for C1/C2/C3 Separation. *Ind Eng Chem Res* 2021;60:4668-4676. [DOI: 10.1021/acs.iecr.0c05916]

8. J. Du, Y. Liu, R. Krishna, et al. Enhancing Gas Sorption and Separation Performance via Bisbenzimidazole Functionalization of Highly Porous Covalent Triazine Frameworks. *ACS Appl Mater Inter* 2018;10:26678-26686. [PMID: 30020769 DOI: 10.1021/acsami.8b08625]

9. J. Yan, B. Zhang and Z. Wang. Highly Selective Separation of CO_2, CH_4, and C2-C4 Hydrocarbons in Ultramicroporous Semicycloaliphatic Polyimides. *ACS Appl Mater Inter* 2018;10:26618-26627. [PMID: 30040370 DOI: 10.1021/acsami.8b07294]

10. Y. Wang, W. Fan, X. Wang, et al. Solvent-induced framework-interpenetration isomers of Cu MOFs for efficient light hydrocarbon separation. *Inorg Chem Front*

2018;5:2408-2412. [DOI: 10.1039/C8QI00469B]

11. J. Zhou, T. Ke, F. Steinke, et al. Tunable Confined Aliphatic Pore Environment in Robust Metal-Organic Frameworks for Efficient Separation of Gases with a Similar Structure. *J Am Chem Soc* 2022;144:14322-14329. [PMID: 35849509 DOI: 10.1021/jacs.2c05448]

12. W. Fan, X. Wang, B. Xu, et al. Amino-functionalized MOFs with high physicochemical stability for efficient gas storage/separation, dye adsorption and catalytic performance. *J Mater Chem A* 2018;6:24486-24495. [DOI: 10.1039/C8TA07839D]

13. D. Wang, T. Zhao, Y. Cao, et al. High performance gas adsorption and separation of natural gas in two microporous metal–organic frameworks with ternary building units. *Chem Commun* 2014;50:8648-8650. [PMID: 24969667 DOI: 10.1039/c4cc03729d]